References and Notes

(1) Bauer, D. R.; Brauman, J. I.; Pecora, R. *Macromolecules* **1975**, *8*, 443.
(2) Basal, B.; Lowry, A.; Yu, H.; Stockmayer, W. H. In "Dielectric Properties of Polymers"; Karasz, F. E., Ed.; Plenum Press: New York, 1972.
(3) Morawetz, H. *Acc. Chem. Res.* **1970**, *3*, 354.
(4) Lauprêtre, F.; Noël, C.; Monnerie, L. *J. Polym. Sci., Polym. Phys. Ed.* **1977**, *15*, 2143.
(5) Valeur, B.; Monnerie, L. *J. Polym. Sci., Polym. Phys. Ed.* **1976**, *14*, 29.
(6) Helfand, E.; Wasserman, Z. R.; Weber, T. A. *J. Chem. Phys.* **1979**, *70*, 2016.
(7) Helfand, E.; Wasserman, Z. R.; Weber, T. A. *Macromolecules* **1980**, *13*, 526.
(8) Weiner, J. H.; Pear, H. R. *Macromolecules* **1977**, *10*, 317.
(9) Fixman, M. *J. Chem. Phys.* **1979**, *69*, 1527, 1538.
(10) Robertas, D. W.; Berne, B. J.; Chandler, D. *J. Chem. Phys.* **1979**, *70*, 3397.
(11) Fixman, M.; Evans, G. T. *J. Chem. Phys.* **1978**, *68*, 195.
(12) Adler, R. S.; Freed, K. F. *J. Chem. Phys.* **1980**, *72*, 2032.
(13) Skolnick, J.; Helfand, E. *J. Chem. Phys.* **1980**, *72*, 5489.
(14) Axelson, D. E.; Levy, G. L.; Mandelkern, L. *Macromolecules* **1979**, *12*, 41.
(15) Dorman, D. E.; Otocka, E. P.; Bovey, F. A. *Macromolecules* **1972**, *5*, 574.
(16) Cudby, M. E. A.; Bunn, A. *Polymer* **1976**, *17*, 345.
(17) Bovey, F. A.; Schilling, F. C.; McCrackin, F. L.; Wagner, H. L. *Macromolecules* **1976**, *9*, 76.
(18) Cheng, H. N.; Schilling, F. C.; Bovey, F. A. *Macromolecules* **1976**, *9*, 363.
(19) Bowmer, T. N.; O'Donnell, J. H. *Polymer* **1977**, *18*, 1032.
(20) Zimm, B. H.; Stockmayer, W. H. *J. Chem. Phys.* **1949**, *17*, 1301.
(21) Orofino, T. A. *Polymer* **1961**, *2*, 305.
(22) Tonelli, A. E. *J. Am. Chem. Soc.* **1972**, *94*, 2972.
(23) Mattice, W. L.; Carpenter, D. K. *Macromolecules* **1976**, *9*, 53.
(24) Mattice, W. L. *Macromolecules* **1978**, *11*, 517.
(25) Solc, K. *Macromolecules* **1973**, *6*, 378.
(26) Mattice, W. L. *Macromolecules* **1977**, *10*, 1182.
(27) Mattice, W. L. *Macromolecules* **1980**, *13*, 506.
(28) Flory, P. J. "Statistical Mechanics of Chain Molecules"; Interscience: New York, 1969.
(29) Blomberg, C. *Chem. Phys.* **1979**, *37*, 219. See also: Brinkman, H. C. *Physica* **1956**, *22*, 149. Landauer, R.; Swanson, J. A. *Phys. Rev.* **1961**, *121*, 1668. Langer, J. S. *Ann. Phys.* **1969**, *54*, 258.
(30) Kramers, H. A. *Physica* **1940**, *7*, 284.
(31) For a comparison with linear alkanes, see Tables II, VII, and VIII of ref 13.
(32) Pitzer, K. S. *Discuss. Faraday Soc.* **1951**, *10*, 66.
(33) Linde, D. R. *J. Chem. Phys.* **1958**, *29*, 1426.
(34) Linde, D. R.; Mann, D. E. *J. Chem. Phys.* **1958**, *29*, 914.
(35) Pitzer, K. S. *J. Chem. Phys.* **1940**, *8*, 711.

Studies on Orientation Behavior of Poly(γ-benzyl L-glutamate) in an Electric Field by means of Small-Angle Light Scattering[1a]

Fumihiko Ozaki,[1b] Tetsuya Ogita,[1b] and Masaru Matsuo*[1c]

Department of Textile Engineering, Faculty of Home Economics, Nara Women's University, Nara 630, Japan, and Department of Textile Engineering, Faculty of Engineering, Yamagata University, Yonezawa 992, Japan.

Received July 23, 1980

ABSTRACT: The orientation behavior of liquid crystalline solutions of poly(γ-benzyl L-glutamate) in chloroform in an electric field was studied by means of small-angle light scattering, the polarizing microscope, and birefringence measurements. The experimental results indicate that the molecular aggregate has a rodlike texture and that the optical axes within the rod are oriented in the electric field direction. In order to study the variation of the light scattering patterns with increasing electric field, we have carried out theoretical calculations by introducing parameters associated with the magnitudes of the optical anisotropy disorder and of the orientation disorder of the optical axes of the scattering elements. Models were proposed in two cases in which the incident beam was parallel and perpendicular to the direction of the electric field. With a proper choice of parameters, the calculated results were found to be rather close to those observed. On this basis, it was concluded that the degree of ordering of the optical axes within the rod increases with increasing electric field.

Introduction

It is well-known that liquid crystals of poly(γ-benzyl L-glutamate) (PBLG) are oriented in electric[2-11] and magnetic fields.[12-16] The orientation behavior has been mainly investigated by means of the polarizing microscope,[2] transient electric birefringence,[10-12] small-angle light scattering,[6,16] and X-ray diffraction techniques.[3,15] Since Robinson[17-19] reported the liquid crystal nature of synthetic polypeptides, these techniques have made clear the orientation behavior of PBLG. Toth and Tobolsky[2] studied the electric orientation of liquid crystalline solutions (15% w/v) of PBLG of molecular weight 310 000 by the polarizing microscope method. They reported that the light transmitted through the sample decreases with increasing electric field when the direction of the incident beam is parallel to the electric field.

Iizuka et al. have studied the orientation behavior of liquid crystalline solutions in electric fields, using small-angle light scattering[6] and infrared dichroic ratios,[4,5] in which the incident beam was perpendicular to the electric field. Wilkes[16] has interpreted the morphology of PBLG films cast from chloroform solutions (that were no older than 1 month) on the basis of the light scattering model proposed by Rhodes and Stein.[20] Using thin films in a 16.5-kG magnetic field, he reported that the molecular clusters, assuming them to have the so-called rodlike texture, were oriented perpendicular to the magnetic field rather than parallel. The theoretical treatment of light scattering from polymer films was developed by Stein, who with his co-workers has reported a number of studies of the small-angle light scattering from unoriented and oriented films[21-24] and from liquid crystals of PBLG.[25,26] They provided a quantitative interpretation[25] of the effect of optical rotation on small-angle light scattering in a system in which polystyrene spherulites were surrounded by an optically active medium consisting of a concentrated

0024-9297/81/2214-0299$01.25/0

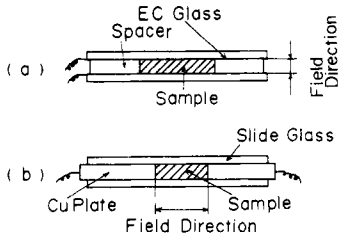

Figure 1. Two cells employed for concentrated solutions of PBLG. (a) A cell constructed from two glass plates whose inner surfaces are made electrically conductive by thin transparent layers of oxide. The electric field direction is parallel to the line of sight through the polarizing microscope and to the beam employed for small-angle light scattering. (b) A cell whose spacing is provided by two Cu plates. The electric field direction is perpendicular to the line of sight through the polarizing microscope and to the beam employed for small-angle light scattering.

solution of PBLG (M_w = 310000) in *m*-cresol (0.15 g/mL).[26]

This paper is concerned with the orientation behavior of liquid crystals of PBLG in chloroform in an electric field as studied by means of the polarizing microscope and small-angle light scattering. The results are discussed on the basis of theoretical calculations of the scattering patterns.

Experimental Procedure

The specimen was a concentrated solution of PBLG with molecular weight 106000 (M_w/M_n = 1.3) and was contained in the cells shown in Figure 1. The concentration of PBLG was about 17 vol % and the experiments were carried out at room temperature. The cell in the form of a capacitor shown in Figure 1a was constructed from two glass plates whose inner surfaces were made electrically conductive by a thin transparent layer of oxide. Spacing was provided by a Teflon sheet through which a window was cut to contain the sample solution. The distance between the two glass plates was 0.2 mm. In this cell, the electric field direction is parallel to the line of sight through the polarizing microscope and to the beam employed for small-angle light scattering. This method was used by Toth and Tobolsky[2] in order to obtain a polarizing photomicrograph of PBLG solutions in the electric field. Figure 1b shows a rectangular cell. A spacing was provided by two Cu plates in the electric field direction and by two Teflon sheets in the other direction perpendicular to the electric field. The distances between the two Cu plates and between the two Teflon sheets are 4 and 10 mm, respectively. The thickness of the Cu plates and of the Teflon sheets must be the same. For the cell shown in Figure 1a, the thickness was 0.2 mm, while for the cell shown in Figure 1b, it was 0.1 mm. In this cell also the electric field direction is perpendicular to the line of sight through the polarizing microscope and to the beam employed for small-angle light scattering. This method was employed by Iizuka et al.[6] to observe the change of light scattering patterns with increasing electric field.

A 3-mW He–Ne gas laser having a wavelength of 6238 Å was used as the light source. The change of birefringence was measured with increasing voltage. In this experiment, the cell shown in Figure 1b was used.

Results and Discussion

We observed the behavior of PBLG in the electric field 30 min after the solution was put in the cell shown in Figure 1a. Figure 2 shows the change of the polarizing photomicrographs with increasing voltage. This result is similar to that obtained by Toth and Tobolsky[2] despite the difference of molecular weight of the samples. The

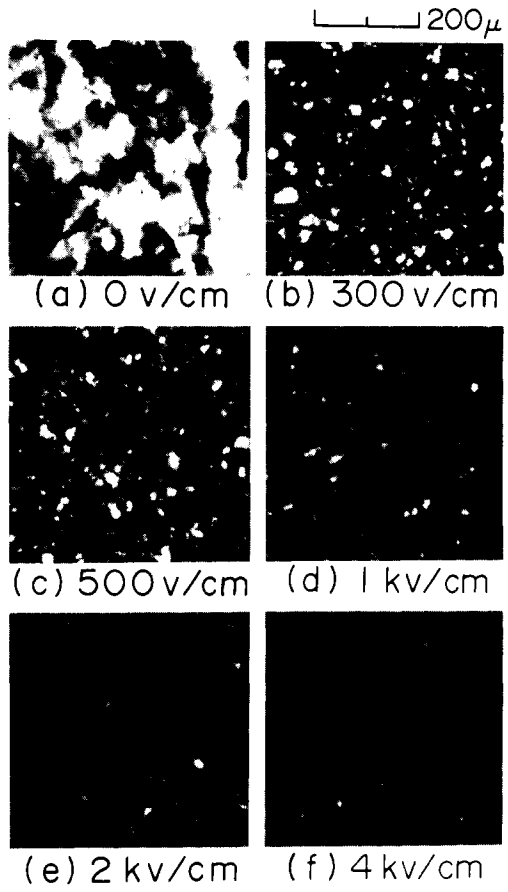

Figure 2. Polarizing photomicrographs with increasing electric field voltage.

birefringent phase exhibits an irregular patchwork of predominantly blue, yellow, and pink regions under crossed polarizers in the absence of an electric field. When the field is applied, one observes a decreasing brightness as the electric field is increased. Figure 2 indicates that the optical axes of the polymer tend to be aligned parallel to the electric field with increasing voltage. Figure 3 shows the H_v light scattering patterns corresponding to Figure 2. Those in parts e and f are typical of an unoriented rodlike texture, while those from the birefringent phase, exhibiting the irregular patchwork, are circular. These results suggest that the X-type patterns are associated with scattering from rodlike textures and that this tendency increases with the degree of darkness observed in the polarizing photomicrographs. This phenomenon seems strange because the light scattering pattern should not appear if the optical axes within the rodlike texture (which is postulated to be a molecular cluster) are perfectly oriented parallel to the electric field. However, we believe this discrepancy may be resolved by introducing an orientation fluctuation of the optical axes of the scattering elements within the rod. Such fluctuations must be introduced to explain the circular type of scattering pattern in the absence of the field. Fluctuation of the orientation of the optical axes was first introduced by Stein and Chu.[27] Subsequently, Stein and Hashimoto published theoretical treatments of the fluctuation of the optical anisotropy of the scattering elements as well as of the orientation of the optical axes in undeformed and deformed spherulites.[28,29] Hashimoto et al.[30] also applied the concept proposed by

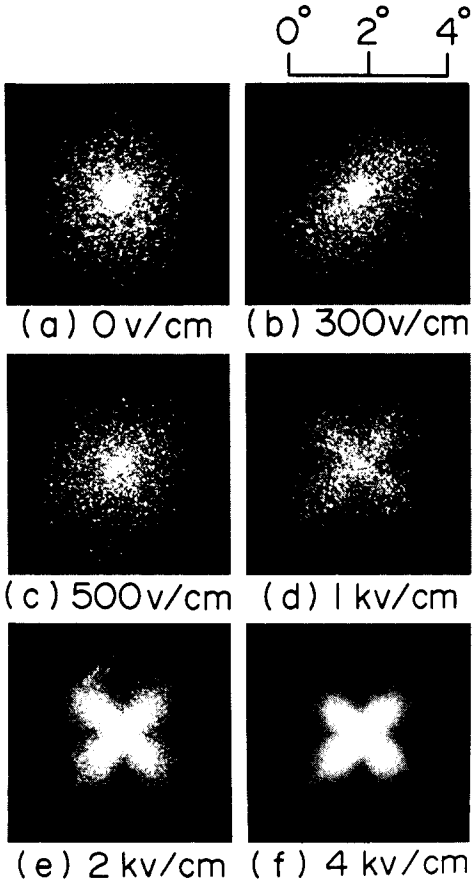

Figure 3. Small-angle light scattering patterns from rodlike textures of PBLG with increasing electric field voltage.

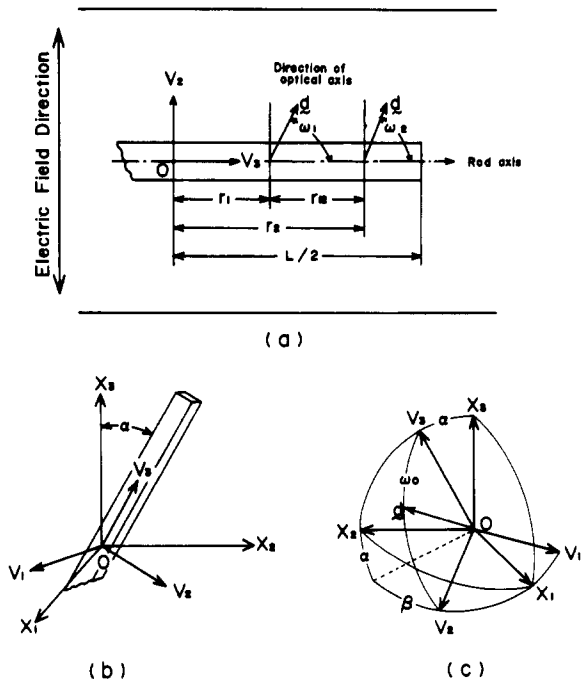

Figure 4. Schematic diagrams of an anisotropic rod with infinitesimally thin lateral dimensions. (a) Optical anisotropy and orientation disorders within the rod with infinitesimally thin lateral dimensions. (b) The rod oriented by the angle α from the vertical direction OX_3 axis in a two-dimensional plane. (c) Cartesian coordinates illustrating the geometrical relations. Eulerian angles α and β specify the orientation of coordinate O–$V_1V_2V_3$ of the structural unit with respect to coordinate O–$X_1X_2X_3$ of the specimen. The angle ω_0 is the polar angle between the optical axis and the V_3 axis.

Stein et al. to disorders of the rodlike textures in polymer films. In this paper, the concept of fluctuations is applied to the scattering patterns from liquid crystal solutions. It appears to be essentially valid. We believe that the extent of the two fluctuations in liquid crystal solutions is remarkable in comparison with the degree of the fluctuation in the solid state.

Figure 4 shows a schematic diagram of an anisotropic rod with infinitesimally thin lateral dimensions. The notation in Figure 4a was previously employed by Hashimoto et al.[30] in investigating the fluctuation of the optical anisotropy and the optical axes within the rod. The angle α represents the orientation of the rod from the vertical axis OX_3 in the plane X_2X_3, as shown in Figure 4b; here, the V_3 axis corresponds to the rod axis and the X_1 axis corresponds to the direction of the incident beam and the electric field. In Figure 4c, the angle β specifies the rotation of the rod around the V_3 axis, that is, the rod axis. When the electric field is applied, the optical axes orient parallel to the X_1 axis. In this system, if β and ω_0 become 90°, the vector **d** denoting the direction of the optical axis conforms to the X_1 direction. This means that the H_v scattering intensity would disappear if it were not for the effect of the orientation fluctuation of the optical axes within the rod. This result indicates that this fluctuation must be considered in order to explain the phenomena appearing in the light scattering patterns in Figure 3 and in the polarizing photomicrographs in Figure 2. In order to carry out the theoretical calculation of light scattering patterns from rodlike textures, it is necessary to consider the size and shape factors of the scattering structures. The results reported in this paper, however, present a difficulty because the size and shape of the scattering structures are not well-defined, as revealed by the polarizing photomicrographs in Figure 2. The rod was therefore assumed to have infinitesimally small lateral dimensions with respect to the wavelength of light in the medium.

According to Rayleigh–Gans theory, the magnitude of light scattering from an anisotropic rod with infinitesimally thin lateral dimensions oriented by an angle α from the vertical direction (OZ) is given by

$$E(\alpha) = C\int_{-L/2}^{L/2}(\mathbf{M}\cdot\mathbf{O})\exp[k(\mathbf{r}\cdot\mathbf{s})]\,d\mathbf{r} \qquad (1)$$

where L is the length of the rod and $\mathbf{r}$ is a vector along the rod axis. C is a constant related to the absolute intensity of scattering and k is defined by $2\pi/\lambda'$, where λ' is the wavelength of light in the medium. The vector $\mathbf{s}$ is defined by $(\mathbf{s}_0 - \mathbf{s}')$, where the vectors $\mathbf{s}_0$ and $\mathbf{s}'$ are unit vectors along the incident and scattered rays, respectively. The vectors **M** and **O** are, respectively, the induced dipole moment of the scattering element located at r in the rod and a unit vector along the polarization direction of the analyzer set perpendicular to the OX_1 axis and in between the sample and the photographic plate used to record the scattering patterns.

After carrying out somewhat complicated calculations by the method described in the Appendix using a method similar to that proposed by Stein et al.[28,29] and Hashimoto et al.,[30] one may obtain the H_v light scattering from rodlike textures disordered with respect to the optical anisotropy and the orientation of the optical axes. The rods are oriented randomly in the two-dimensional plane and the rotation of a rod is associated with the distribution function $N(\beta)$, discussed later. The H_v light scattering intensity may then be written as follows:

$$I_{H_v} = \int_0^{2\pi} E(\alpha)E^*(\alpha)\,d\alpha$$
$$= \frac{C'\delta_0^2}{16}\Big[\int_0^{2\pi}(\Omega_1 \sin^2 2\alpha + 4\Omega_2 \cos^2 2\alpha + \Omega_3 \sin^2 2\alpha)\int_0^L (L - r_{12})\{1 + A\Psi(r_{12})\}f(r_{12}) \times \cos(br_{12})\,dr_{12}\,d\alpha + \int_0^{2\pi}(\Omega_3 + \Omega_4) \times \sin^2 2\alpha \int_0^L (L - r_{12})\{1 + A\Psi(r_{12})\}\cos(br_{12})\,dr_{12}\,d\alpha\Big] \quad (2)$$

where

$$\Omega_1 = \{\cos^2 2\omega_0\langle\cos^2 2\Delta_1\rangle_{av} + \sin^2 2\omega_0\langle\sin^2 2\Delta_1\rangle_{av}\}\int_0^{2\pi} N(\beta)(1 + \cos^2\beta)^2\,d\beta \quad (3)$$

$$\Omega_2 = \{(1 - 2\cos^2 2\omega_0) \times \langle\cos^2 2\Delta_1\rangle_{av} + \cos^2 2\omega_0\}\int_0^{2\pi} N(\beta)\cos^2\beta\,d\beta \quad (4)$$

$$\Omega_3 = \cos 2\omega_0\langle\cos 2\Delta_1\rangle_{av}\int_0^{2\pi} N(\beta)(1 - \cos^4\beta)\,d\beta \quad (5)$$

$$\Omega_4 = \int_0^{2\pi} N(\beta)\sin^4\beta\,d\beta \quad (6)$$

Here, $r_{12} = r_2 - r_1$ and δ_0 is the optical anisotropy of the scattering element defined by $(\alpha_\parallel - \alpha_\perp)$, which is assumed to be uniaxially symmetrical with polarizabilities $\alpha_\parallel$ and $\alpha_\perp$ along and perpendicular to the optical axis. $\Psi(r_{12})$ and $f(r_{12})$ are the correlation functions for the internal anisotropy and the orientation fluctuations, respectively, and are defined by

$$\Psi(r_{12}) = \langle\Delta\delta_1\Delta\delta_2\rangle_{r_{12}}/\langle(\Delta\delta_1)^2\rangle_{av} \quad (7)$$

$$f(r_{12}) = \langle\cos 2\Delta_{12}\rangle_{r_{12}} \quad (8)$$

The quantity Δ_{12} is defined by $\Delta_{12} = \Delta_2 - \Delta_1 = \omega_2 - \omega_1$, the angle characterizing the relative orientation of the optical axes of two scattering elements separated by a distance r_{12}. The quantities $\langle(\Delta\delta_1)^2\rangle_{av}$ and $\langle\cos^2 2\Delta_1\rangle_{av}$ (or $\langle\sin^2 2\Delta_1\rangle_{av}$) are parameters associated with the magnitudes of the anisotropy and orientation disordering. The quantity A is defined by $\langle(\Delta\delta_1)^2\rangle_{av}/\delta_0^2$, which is associated with the relative magnitude of the anisotropy fluctuation. The quantity b, which is a function of the scattering angle θ, the azimuthal angle μ, and the angle α shown in Figure 4, is given by

$$b = -\frac{2\pi}{\lambda'}\sin\theta\cos(\alpha - \mu) \quad (9)$$

Following Hashimoto et al.,[30] the effects of the anisotropy and orientation disorders are considered separately. The correlation functions, which, in general, decrease asymptotically from unity to zero with increasing distance $|r_{12}|$ from zero, were assumed to be given by the empirical functions

$$\Psi(r_{12}) = \exp(-|r_{12}|/a) \quad (10)$$

$$f(r_{12}) = \exp(-|r_{12}|/c) \quad (11)$$

where a and c are the correlation distances. This method was first proposed in connection with the problem of an undeformed spherulite by Stein and Chu[27] and applied to the problem of a rod by Hashimoto et al.[30] The two parameters, the correlation distance and the magnitude of the fluctuation, are expected to be interrelated for a particular model of the fluctuating system, as discussed by Stein and Chu[27] for the undeformed spherulite. The

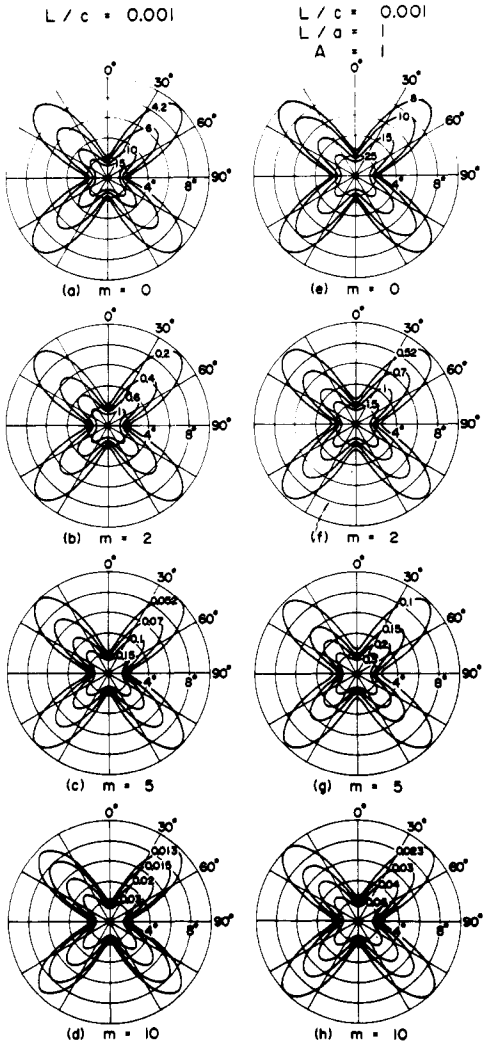

Figure 5. Small-angle light scattering patterns calculated from eq 2.

interrelating equation derived by Stein and Chu[27] was used in treating the orientation fluctuation of the rod by Hashimoto et al.[30] The same method was used in this study and therefore $\langle\cos^2 2\Delta_1\rangle_{av}$ may be given by

$$\langle\cos^2 2\Delta_1\rangle_{av} = \frac{1}{2} - \frac{1}{16(L/c)^2}[1 - 4(L/c) - \exp(-4L/c)] \quad (12)$$

This reduces to $^1/_2$ as c approaches zero, corresponding to completely random fluctuations. On the other hand, the value reduces to unity as c becomes large, corresponding to no internal disorder. Moreover, $\langle\cos 2\Delta_1\rangle_{av}$ may be given by

$$\langle\cos 2\Delta_1\rangle_{av} = \frac{2}{(L/c)^2}[L/c - 1 + \exp(-L/c)] \quad (13)$$

This reduces to zero as c approaches zero and to unity as c becomes large.

$N(\beta)$ is the orientation distribution function for the rotation of the rod around its own axis and is given by

$$N(\beta) = \frac{1}{2\pi}\sin^{2m}\beta \quad (14)$$

If m approaches infinity, the optical axes are oriented in the V_3V_1 plane, while if m is equal to zero, the rod exists in the X_2X_3 plane and is rotated randomly around its own axis.

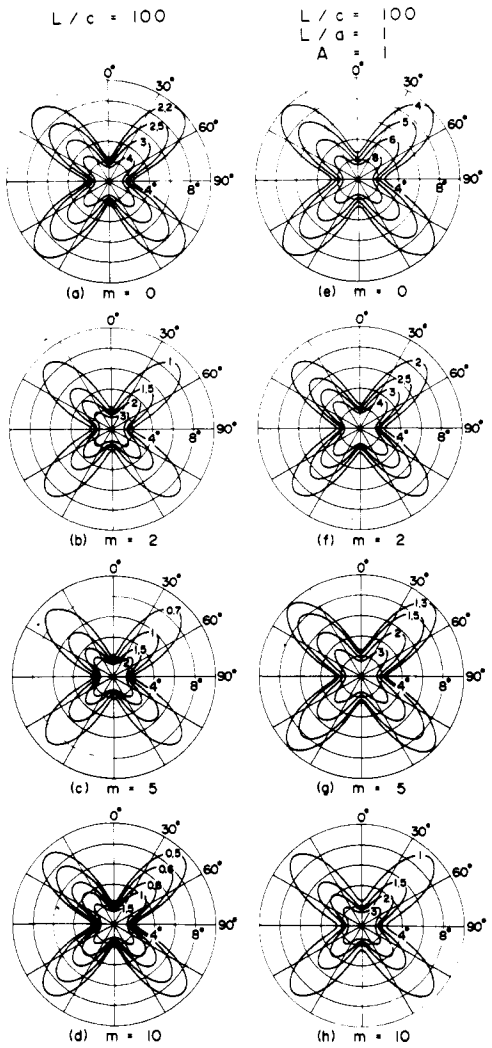

Figure 6. Small-angle light scattering patterns calculated from eq 2.

The results of numerical calculations are shown in Figures 5 and 6 at $L/\lambda' = 40$. The values of the correlation distance specified by L/c were 0.001 and 100 in Figures 5 and 6, respectively; the first value is associated with a small disorder of the orientation of the optical axes, and the second with a large disorder. The scattering patterns in the two figures are shown as a function of the parameter m associated with the rotation mode of the rod around its own axis. The patterns on the right side of Figures 5 and 6 were calculated by taking account of the effect of the correlation distance specified by L/c, while those on the left side were calculated by taking into account the effect of the optical anisotropy fluctuation with the correlation distance for two given parameters L/a and A in addition to the effect of the correlation distance L/c. The scattering patterns are of the X type despite the change of the values of m and L/c and are close to the experimental patterns at the higher voltages (2 and 4 kV/cm). If the polar angle ω_0 of the optical axes is fixed at 90° with respect to the rod axis without orientation disorder and m is infinite, the optical axes conform to the electric field direction, that is, the direction of the incident beam. The intensity of H_v light scattering therefore becomes zero. Hence, in order to explain the orientation behavior of the optical axes in the electric field, we must assume that the polar angle ω_0 is equal to 90° and the parameter m is very large in this model. From the observed decrease of light transmitted when the electric field is applied, one may postulate that

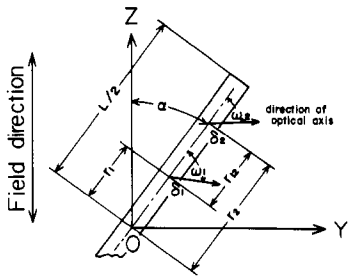

Figure 7. Schematic diagram of an anisotropic rod with infinitesimally thin lateral dimensions. The optical axes and the rod axis are in the same plane.

the optical axes orient predominantly parallel to the direction of the incident beam with increasing voltage.

According to the patterns shown in Figures 5 and 6, increasing values of m correspond to decreasing scattering intensity. This result indicates that the intensity has a maximum value in the random rotation of the rod around its own axis, which is independent of the value of the correlation distance L/c denoting the degree of orientation disorder of the optical axes within the rod. Moreover, increasing the correlation distance L/c causes an increase of intensity at fixed values of m when $m \geq 2$. This relationship is contrary to the case when $m = 0$. The influence of L/c in increasing the intensity becomes significant when the O–V_3V_2 plane coincides with the O–X_1X_3 plane. This result is reasonable when one considers the orientation of the optical axes. The optical axes conform to the direction of the incident beam when L/c is zero and m is infinite, and consequently the intensity becomes zero. On the other hand, an increase of the orientation fluctuation of the optical axes causes a decreased intensity in the case of random rotation of the rod around its own axis. The μ dependence of the intensity is found to be hardly affected by the value of L/c and, moreover, the shape of the scattering pattern is found to be hardly affected by the optical anisotropy disorder. The scattering patterns on the right side in Figures 5 and 6 are shown as examples of cases where $L/a = 1$ and $A = 1$. The scattered intensity increases upon introduction of disorder in optical anisotropy.

Upon comparing the calculated results in Figures 5 and 6 with the experimental results in Figure 3, we see that all the calculated patterns are of the X type, while the observed patterns become the X type at voltages beyond 1 kV/cm but are of the circular type at voltages below 500 V/cm. This result suggests that the model in Figure 4 may explain the orientation behavior of the rods at higher voltages but does not suffice to explain it at lower voltages. We therefore propose another model to explain the circular patterns.

Figure 7 shows the schematic diagram of an anisotropic rod; the optical axes and the rod axis are in the O–YZ plane. The rod is not allowed to rotate around its own axis. For this system, Hashimoto et al.[30] show that

$$I_{H_v} = \frac{C}{8\pi^2}\delta_0^2\Big[\int_0^{2\pi}\{\sin^2 2(\xi+\mu+\omega_0)\langle\cos^2 2\Delta_1\rangle_{av} + \cos^2 2(\xi+\mu+\omega_0)\langle\sin^2 2\Delta_1\rangle_{av}\}\int_0^L (L-r_{12})\times \{1+A\Psi(r_{12})\}f(r_{12})\cos\{-(2\pi/\lambda')\sin\theta\cos\xi\}\,dr_{12}\,d\xi\Big] \quad (15)$$

where

$$\xi = \alpha - \mu \quad (16)$$

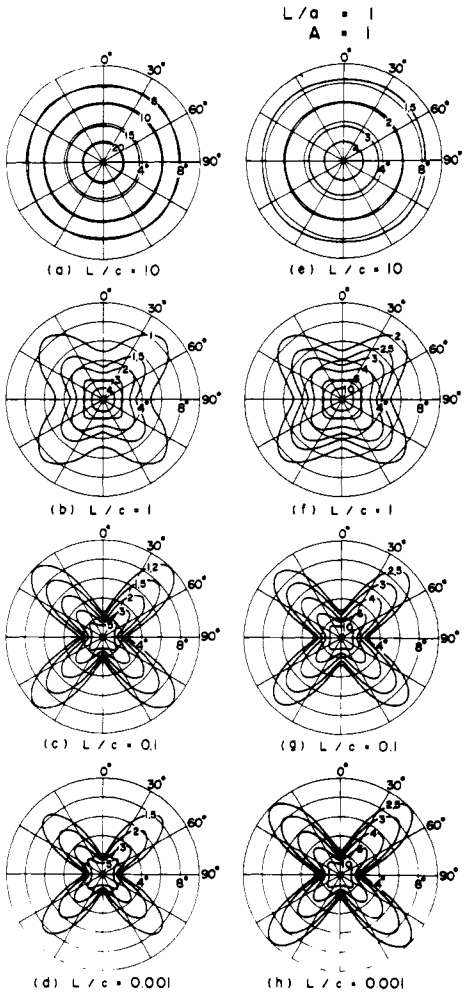

Figure 8. Light scattering patterns calculated from eq 15.

In eq 15, if the orientation of optical axes is completely random fluctuation, $\langle \cos^2 2\Delta_1 \rangle_{av}$ and $\langle \sin^2 2\Delta_1 \rangle_{av}$ are equal to $^1/_2$, and therefore eq 15 may be rewritten as follows:

$$I_{H_v} = \frac{C}{8\pi^2}\delta^2\Big[\int_0^{2\pi}\int_0^L (L - r_{12})\{1 + A\Psi(r_{12})\}f(r_{12}) \times \cos\{-(2\pi/\lambda')\sin\theta\sin\xi\}\, dr_{12}\, d\xi\Big] \quad (17)$$

Equation 17 is not a function of μ and ω_0; that is, the scattering pattern for completely random fluctuations becomes circular and is independent of the polar angle of the optical axes with respect to the rod axis. Figure 8 shows the patterns calculated as a function of L/c at $\omega_0 = 0°$. The patterns on the right side were calculated by taking into account the effect of the correlation distance, specified by L/c, while those on the left side were calculated by taking into account the effect of the optical anisotropy fluctuation with the correlation distance for two given parameters L/a and A, in addition to the correlation distance L/c. As can be seen in Figure 8, the scattering pattern changes from circular to X type with decreasing values of L/c, that is, with decreasing disorder of the optical axes. This result does not contradict the assumptions involved in eq 15 and 17. The μ dependence of the intensity decreases with increasing values of L/c. At larger values of θ, this tendency becomes strong. The optical anisotropy fluctuation is hardly affected by the shape of the scattering patterns but increases the scattered intensity. In addition, the actual calculation was carried out for 0 and 90° values of ω_0 and consequently the shapes of the patterns calculated at $\omega_0 = 0°$ were found to be quite similar to those calculated at $\omega_0 = 90°$, although the scattered intensities of the patterns are a little different. However, we may postulate that the polar angle ω_0 is equal to 0° because of the nematic nature of the liquid crystals of PBLG in this experiment. The results calculated at $\omega_0 = 0°$ for the model shown in Figure 7 are rather close to the patterns observed for larger values of L/c such as 10. This result suggests that the disorder of the orientation fluctuation of the optical axes within the rod is strong in the absence of the applied field but that the rod rotates little around its own axis. Hence, we believe that when the electric field is applied, the optical axes conforming to the rod axis orient parallel to the field, and consequently the polar angle ω_0 changes from 0 to 90° without rotation of the rod.

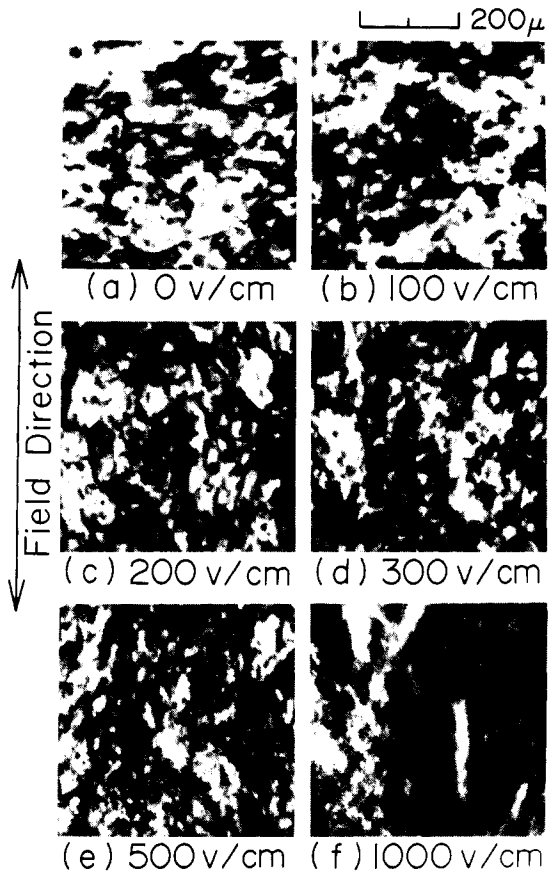

Figure 9. Polarizing photomicrographs of the orientation behavior of the PBLG rodlike texture with increasing electric field voltage.

From the calculated scattering patterns, it appears that the orientation of the rods may be explained by the model shown in Figure 7 in the absence of an applied field and by the model shown in Figure 4 at larger values of m and $\omega_0 = 90°$ when the electric field is applied. Actually, the patterns calculated at $m = 10$ were found to be nearly the same as the patterns calculated at $\beta = 90°$ in Figure 4c.

In this paper, an additional method was used to investigate the behavior of the molecular clusters of PBLG, that is, the rodlike texture, in an electric field. The cell shown in Figure 1b was used. In this experiment, the flow of the rods in the direction of the electric field may be clearly observed. As the voltage was increased, the rods flowed with increasing velocity. The behavior was recorded with a television camera and video recorder. Figure 9 shows the polarizing photomicrographs reproduced on the television, from which one may confirm the preferential orientation of the rods parallel to the electric field.

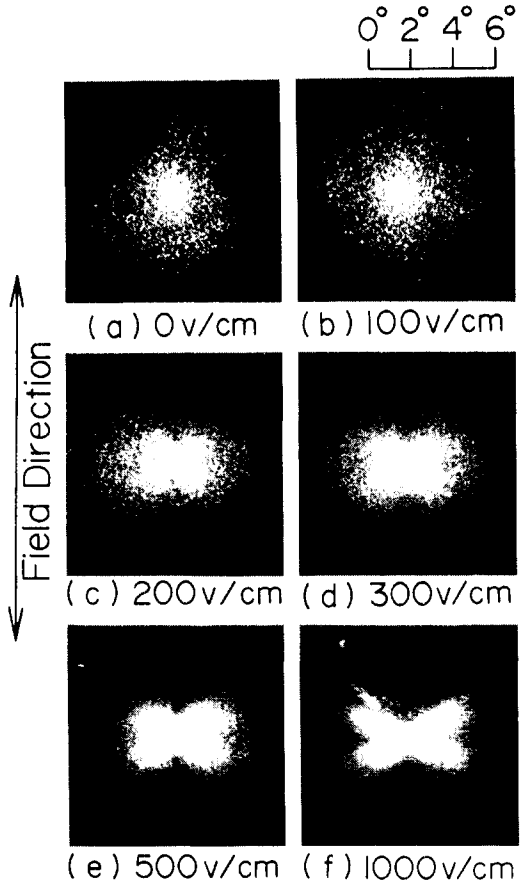

Figure 10. Small-angle light scattering patterns from rodlike textures of PBLG with increasing electric field voltage.

Figure 10 shows H_v light scattering patterns corresponding to the polarizing photomicrographs in Figure 9. The scattering pattern changes from circular to X type with increasing voltage. Beyond 500 V/cm, the four lobes are extended in the horizontal direction. This result suggests that the shearing stresses produced in the cell do not destroy the rodlike texture and are sufficient to promote the preferential orientation of the rods in the electric field direction. Moreover, these stresses decrease the orientational disorder of the optical axes with respect to the rod axis.

We also measured the birefringence with change of voltage in order to investigate the direction of orientation of the optical axes with respect to the electric field. Figure 11 shows the positive birefringence in the electric field direction. There is an increase with voltage but beyond 250 V/cm, it tends to level off. These were obtained by allowing 15 min at each setting to obtain a relatively stable reading of the compensator. This result indicates that the preferred orientation of the optical axes is in the electric field direction.

As discussed above, the H_v light scattering and birefringence measurements suggest that the optical axes within the rod, as well as the rods themselves, tend to orient preferentially parallel to the electric field. The observed intensity of H_v light scattering shown in Figure 10 does not decrease very much even at 1000 V/cm. This result is quite different from that obtained by Iizuka et al.,[6] who found that the intensity of V_h scattering was almost equivalent to H_v scattering in this system, becoming weaker with increasing ordering of the liquid crystalline CH_2Br_2 solution of PBLG at voltages beyond 281 V/cm. This different result seems to arise from two factors, one associated with the magnitude of the orientation fluctuation of the optical axes oriented at polar angle $\omega_0 = 0°$ with respect to the rod axis and the other associated with the orientation distribution of the rods with respect to the electric field direction. One may presume that the fluctuations of the optical axes for the specimen used in this experiment are larger and also that the shape of the distribution function of the rods is broader compared to those of the specimen used by Iizuka et al.[6] We note again that the scattered intensity becomes zero when the orientation disorder of the optical axes is zero and the rods are oriented perfectly parallel to the electric field. The discrepancy between our results and those of Iizuka et al.[6] seems to arise from a difference in molecular weight as well as in the concentration of the solutions.

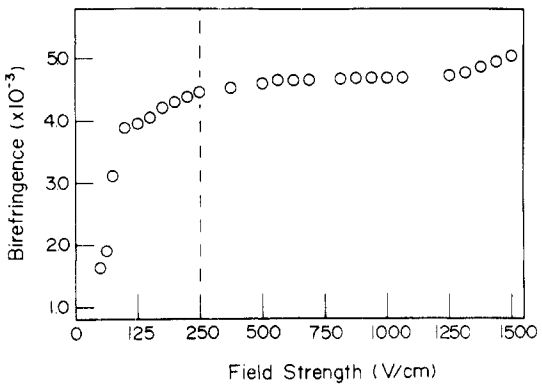

Figure 11. Change of birefringence with increasing electric field voltage.

The H_v light scattering intensity from rods having optical anisotropy and orientation disorder of the optical axes, which are oriented by an angle α in a two-dimensional plane, may be calculated in a manner similar to eq 15:

$$I_{H_v} = \frac{C\delta_0^2}{16}\int_0^{2\pi} N(\alpha)\{\sin^2 2(\alpha + \omega_0)\langle\cos^2 2\Delta_1\rangle_{av} + \cos^2 2(\alpha + \omega_0)\langle\sin^2 2\Delta_1\rangle_{av}\}\int_0^L (L - r_{12})\{1 + A\Psi(r_{12})\}f(r_{12})\cos(br_{12})\,dr_{12}\,d\alpha \quad (18)$$

where $N(\alpha)$ is the orientation function of the rods. This may be expressed by assuming an affine orientation in the two-dimensional plane as follows:

$$N(\alpha) = \lambda^4/\{\lambda^4 - (\lambda^4 - 1)\cos^2\alpha\} \quad (19)$$

where the parameter λ essentially defines the degree of orientation. The affine orientation in a three-dimensional space was invoked by Iizuka et al.[6] to explain the orientation behavior of the rodlike texture of PBLG in chloroform in an electric field. The value of the angle ω_0 is presumed to be 0° from the positive birefringence in the electric field direction. This does not contradict the results discussed above for eq 15 in the absence of the electric field. In this calculation, the elongation of the rod by shearing stresses is neglected.

The results of numerical calculations are shown in Figures 12–14, in which a–d were calculated from the effect of the orientation fluctuation of the optical axes within the rod, while e–h were calculated by introducing the effect of the optical anisotropy in addition to the orientation fluctuation. The former calculations were carried out with the various correlation distances specified by L/c, while the latter calculations were carried out with various values of L/c for the parameters fixed at $L/a = 1$ and $A = 1$. As shown in Figures 13 and 14, at $\lambda = 2.0$ and 3.0, an increase of the orientation disorder increases the scattered intensity, while at $\lambda = 1.5$ it decreases it as shown in Figure 12. The

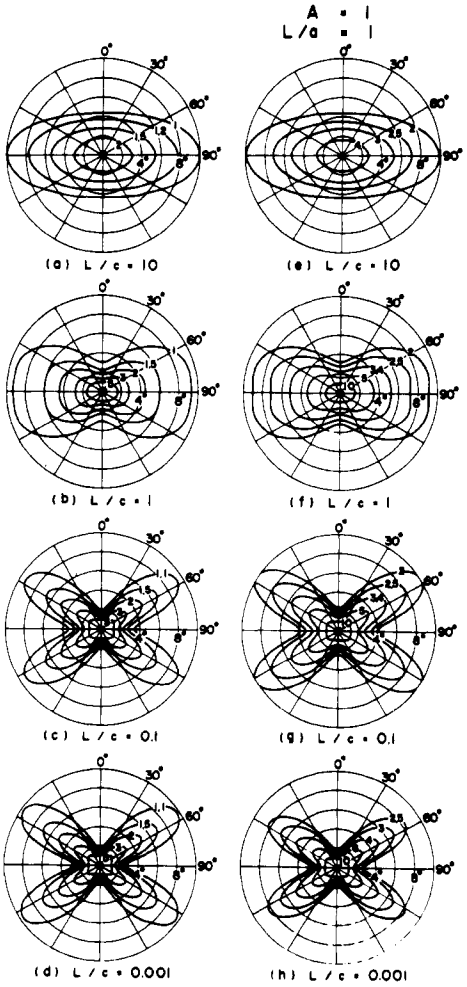

Figure 12. Small-angle light scattering patterns calculated from eq 17 for the case $\lambda = 1.5$.

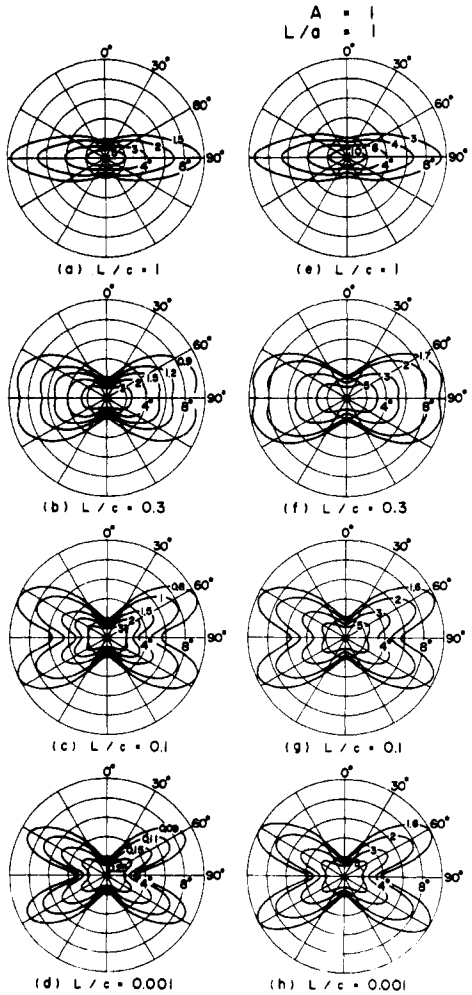

Figure 13. Small-angle light scattering patterns calculated from eq 17 for the case $\lambda = 2.0$.

μ dependence of the intensity decreases with an increase in the orientation fluctuation. The optical anisotropy was found to be hardly dependent on the shape of the scattering patterns from the results calculated with various values of the parameters L/a and A, although the scattered intensity increases upon introducing these parameters. The results calculated at $L/a = 1$ and $A = 1$ are shown on the right side of Figures 12–14. The patterns shown in Figures 12–14 suggest that the effect of the orientation fluctuation upon the scattering patterns is much greater than the effect of the anisotropy disorder. The four scattering lobes are extended in the horizontal direction with increasing values of λ, the degree of rod orientation. The scattering patterns shown in Figures 12–14 were calculated for the cases $\lambda = 1.5$, 2.0, and 3.0, respectively, as discussed above. The extension of the scattering lobes in the horizontal direction with increasing λ was reported by Stein et al.[20] and Hashimoto et al.[31] The patterns calculated at the smaller values of L/c, i.e., 0.1 and 0.001, are rather close to the observed results when proper values of λ are used. This agreement suggests that the degree of ordering of liquid crystalline solutions of PBLG in chloroform increases with increasing field.

We also investigated the hysteresis of the orientation behavior of PBLG in an electric field. Half an hour after an electric field of 1000 V/cm was cut off, the field was applied again. Figure 15 shows the change of the scattering patterns observed in the process. The patterns in Figure 15 became clearly of the X type beyond 200 V/cm, similarly to the patterns in Figure 10 beyond 500 V/cm. Thus, the scattering patterns exhibit hysteresis. We also found that the electric current through the solution exhibits hysteresis. Figure 16 shows the results of successive measurements carried out at 0.5-h intervals. The electric current diminishes after each interval. It is probable that this result is related to the differences in the scattering patterns with increasing voltage shown in Figures 10 and 15. However, detailed understanding has not yet been achieved.

When the first measurement was finished and the electric field (1000 V/cm) was cut off, the light scattering pattern was destroyed and after 10 min the pattern became of the X type. Figure 17 shows the scattering pattern and the corresponding polarizing photomicrograph. After a further 5 min, however, the pattern began to disappear and to become circular, as shown in Figure 10a. The cause of the X type pattern under these circumstances also remains an unresolved problem.

Figure 18 shows the light scattering patterns for a film cast from a chloroform solution used in this paper. The patterns were obtained from the same sample and at the same location by rotation of the sample. The difference between these patterns must be due to the effect of the local orientation rather than to the effect of optical rotation, as suggested by Wilkes.[16] If the difference were due to the effect of optical rotation, the scattering pattern would not change upon rotation of the sample. This problem seems worth investigating, although the mechanism in the process from solutions to films is not discussed in this paper.

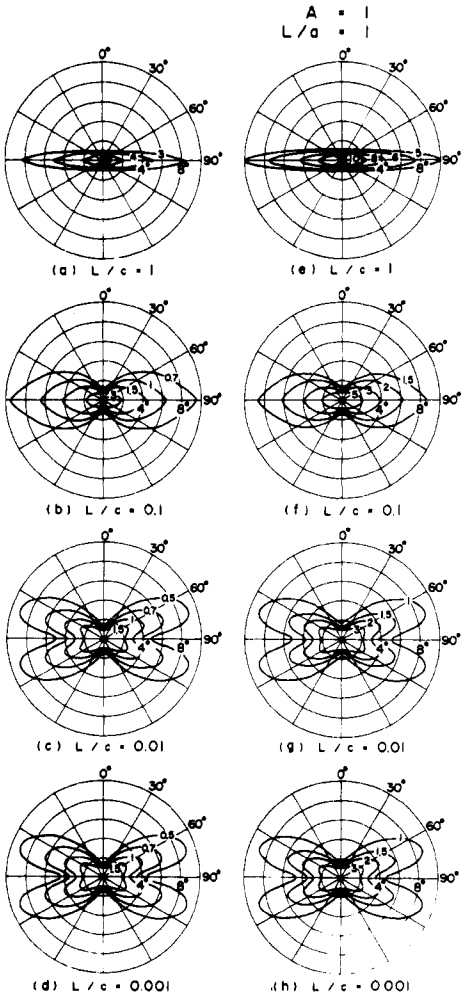

Figure 14. Small-angle light scattering patterns calculated from eq 17 for the case $\lambda = 3.0$.

Conclusions

The orientation behavior of liquid crystals of PBLG in chloroform solutions in an electric field was investigated by means of the polarizing microscope and small-angle light scattering. A concentrated chloroform solution of PBLG of molecular weight 106 000 ($M_w/M_n = 1.3$) was used as a specimen, the concentration being about 17 vol %. The birefringent phase under the polarizing microscope exhibited an irregular patchwork of predominantly blue, yellow, and pink regions without applying the electric field under the crossed polarizers. The experiments were carried out in the two cases that the incident beam was parallel and perpendicular to the direction of the electric field:

(1) When the electric field was applied parallel to the incident beam, the brightness decreased with increasing electric field. The H_v light scattering patterns from the birefringence phase, exhibiting the irregular patchwork, are circular without applying the electric field, whereas when the applied voltage is increased, the scattering patterns became a typical X type of an unoriented rodlike texture. In order to analyze the variation of the scattering patterns with increasing electric field, the theoretical calculations were made for a model system by introducing the parameters associated with the magnitudes of the optical anisotropy disorder and of the orientation disorder of the optical axes of the scattering element. In this model system, rods orient randomly in the two-dimensional plane, the optical axes being fixed with respect to the rod axis at a polar angle of 90°. When the electric field is applied,

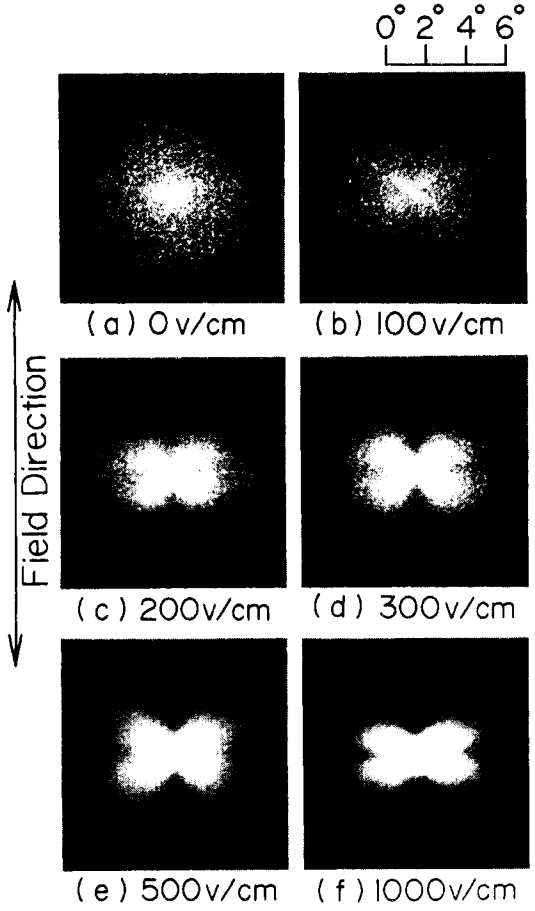

Figure 15. Change of the small-angle light scattering patterns observed in an electric field. The electric field was applied 1 h after the first measurement was finished and the voltage at 1000 V/cm had been cut off.

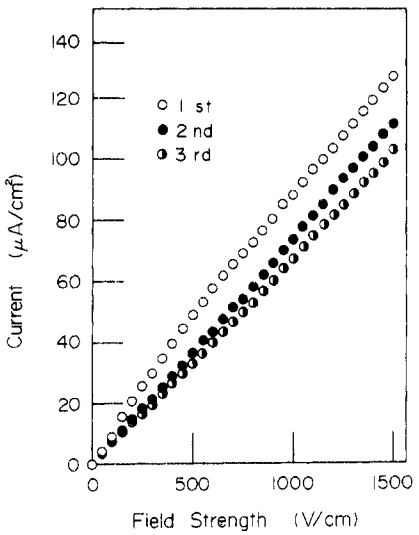

Figure 16. Electric current through the solutions of PBLG enclosed in the cell taken in the electric field.

the rod rotates around its own axis to orient the optical axes to the electric field. The results calculated for the above model were rather close to those observed at the high voltages of 2 and 4 kV/cm. However, such a theoretical treatment does not provide an explanation for the orientation behavior of the rods at voltages lower than 500 V/cm. Thus, another model is proposed to explain the circular patterns, the optical and rod axes being in the two-dimensional plane and the rod not being allowed to

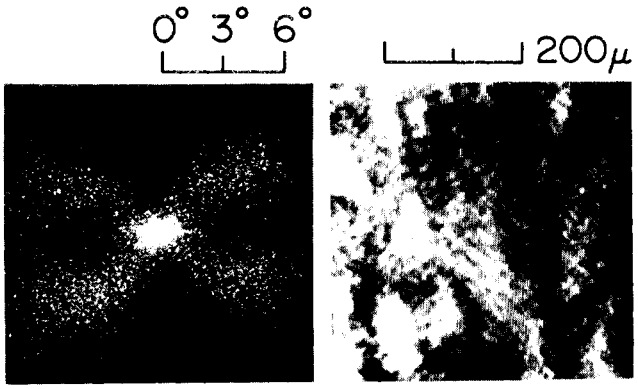

Figure 17. Small-angle light scattering pattern and polarizing photomicrograph obtained 10 min after the first measurement was finished and the electric field was cut off.

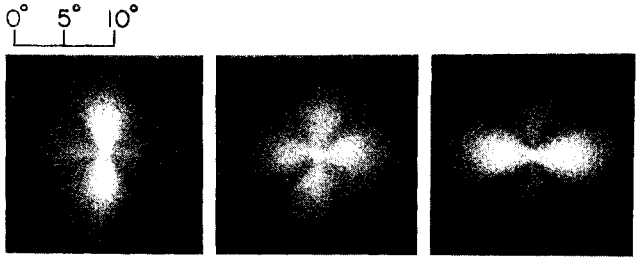

Figure 18. Small-angle light scattering patterns obtained upon rotation of a PBLG film at the same location.

rotate around its own axis. When the proper parameters of the orientation disorder are chosen, the calculated results became fairly close to the patterns observed.

(2) *When the electric field was applied perpendicular to the incident beam*, the flow of the rods in the direction of the electric field was well observed by the polarizing microscope. The scattering pattern changed from circular to X type with increasing voltage. At voltages larger than 500 V/cm, the four lobes are extended in the horizontal direction. This suggests that the shearing stresses produced in the cell do not destroy the rodlike texture and sufficiently promote the preferential orientation of the rods in the electric field. Moreover, the stresses decreased the orientational disorder of the optical axes with respect to the rod axis. The behavior was accounted for by the orientation of rods, the optical and rod axes being in the two-dimensional plane and the rod orienting in the electric field in an affine mode without rotation around its own axis. When the proper parameters of the orientation disorder were chosen, the calculated results became satisfactorily close to the patterns observed.

Judging from the results calculated, the optical anisotropy fluctuation was hardly dependent on the shape of the scattering patterns, though the scattered intensity increased with use of the parameters.

Acknowledgment. We thank Dr. Hayashi and Professor Nakajima, Department of Polymer Chemistry, Faculty of Engineering, Kyoto University, for the sample used and for their valuable comments and suggestions. Thanks are also due to Professor Kawai, Department of Polymer Chemistry, Faculty of Engineering, Kyoto University, and Professor Kimura, Department of Chemistry, Faculty of Science, Nara Women's University, for their helpful comments.

Appendix

Considering the schematic diagram shown in Figure 4, one obtains the vectors of three principal axes of the rodlike texture by

$$\mathbf{V}_3 = \cos\alpha\mathbf{k} + \sin\alpha\mathbf{j}$$
$$\mathbf{V}_2 = -\cos\beta\sin\alpha\mathbf{k} + \cos\beta\cos\alpha\mathbf{j} + \sin\beta\mathbf{i} \quad \text{(A-1)}$$
$$\mathbf{V}_1 = \sin\beta\sin\alpha\mathbf{k} - \sin\beta\cos\alpha\mathbf{j} + \cos\beta\mathbf{i}$$

where $\mathbf{k}$, $\mathbf{j}$, and $\mathbf{i}$ are unit vectors along the $\mathbf{X}_1$, $\mathbf{X}_2$, and $\mathbf{X}_3$ axes, respectively. The vector of optical axis $\mathbf{d}$ may be given by

$$\mathbf{d} = \cos\omega\mathbf{V}_3 + \sin\omega\mathbf{V}_2$$
$$= (\cos\omega\cos\alpha - \sin\omega\cos\beta\sin\alpha)\mathbf{k} + (\cos\omega\sin\alpha + \sin\omega\cos\beta\cos\alpha)\mathbf{j} + \sin\omega\sin\beta\mathbf{i} \quad \text{(A-2)}$$

Thus, $(\mathbf{M}\cdot\mathbf{O})$ for the H_v polarization may be given by

$$(\mathbf{M}\cdot\mathbf{O}) = \tfrac{1}{4}\{(1+\cos^2\beta)\sin 2\alpha\cos 2\omega + \sin^2\beta\sin 2\alpha + 2\sin 2\omega\cos 2\alpha\cos\beta\} \quad \text{(A-3)}$$

By using eq 1, we write the H_v scattered intensity as

$$I_{H_v}(\alpha) = \frac{C'}{2\pi}\int_{\beta=0}^{2\pi}\int_{-L/2}^{L/2}\int_{-L/2}^{L/2}\delta_1\delta_2(\mathbf{M}\cdot\mathbf{O})_1(\mathbf{M}\cdot\mathbf{O})_2 \times \exp[-k(\mathbf{r}_1\cdot\mathbf{s})]\exp[k(\mathbf{r}_2\cdot\mathbf{s})]\,d\mathbf{r}_1\,d\mathbf{r}_2\,d\beta \quad \text{(A-4)}$$

Assuming $r_2 \geq r_1$, we rewrite eq A-4 as

$$I_{H_v}(\alpha) = \frac{C'}{2\pi}\int_{\beta=0}^{2\pi}\int_0^L\left[\int_{-L/2}^{L/2-r_{12}}d\mathbf{r}_1\right]\delta_1\delta_2 \times (\mathbf{M}\cdot\mathbf{O})_1(\mathbf{M}\cdot\mathbf{O})_2\cos[k(\mathbf{r}_{12}\cdot\mathbf{s})]\,d\mathbf{r}_{12}\,d\beta$$
$$= \frac{C'}{2\pi}\int_\beta^\pi\int_0^L(L-r_{12})\delta_1\delta_2 \times (\mathbf{M}\cdot\mathbf{O})_1(\mathbf{M}\cdot\mathbf{O})_2\cos(br_{12})\,dr_{12}\,d\beta \quad \text{(A-5)}$$

where

$$k(\mathbf{r}_{12}\cdot\mathbf{s}) = -\frac{2\pi}{\lambda'}\sin\theta\cos(\alpha-\mu)r_{12} = br_{12} \quad \text{(A-6)}$$

According to a method proposed by Hashimoto and Stein,[28] we have

$$\langle\delta_1\,\delta_2\rangle_{r_{12}} = \delta_0^2\{1 + A\Psi(r_{12})\} \quad \text{(A-7)}$$

The average $\langle(\mathbf{M}\cdot\mathbf{O})_1(\mathbf{M}\cdot\mathbf{O})_2\rangle_{r_{12}}$ may be calculated by using a method similar to that proposed by Stein and Chu,[27] which may be given by

$$\langle(\mathbf{M}\cdot\mathbf{O})_1(\mathbf{M}\cdot\mathbf{O})_2\rangle_{r_{12}} =$$
$$\tfrac{1}{16}[(1+\cos^2\beta)^2\{\cos^2 2\omega_0\langle\cos^2 2\Delta_1\rangle_{av} + \sin^2 2\omega_0\langle\sin^2 2\Delta_1\rangle_{av}\}\langle\cos 2\Delta_{12}\rangle\sin^2 2\alpha + 4(1+\cos^2\beta)\cos\beta\sin 2\omega_0 \times \cos 2\omega_0(2\langle\cos^2 2\Delta_1\rangle_{av} - 1)\langle\cos 2\Delta_{12}\rangle_{av}\sin 2\alpha\cos 2\alpha + 4\cos^2\beta\{(1-2\cos^2 2\omega_0)\langle\cos^2 2\Delta_1\rangle_{av} + \cos^2 2\omega_0\}\langle\cos 2\Delta_{12}\rangle_{av}\cos^2 2\alpha - (1-\cos^4\beta)\cos 2\omega_0\langle\cos 2\Delta_1\rangle_{av}\sin^2 2\alpha + \sin^2\beta\cos\beta\sin 2\omega_0\langle\cos 2\Delta_1\rangle_{av}\cos 2\alpha\sin 2\alpha + (1-\cos^4\beta)\cos 2\omega_0\langle\cos 2\Delta_1\rangle_{av}\langle\cos 2\Delta_{12}\rangle_{av}\sin^2 2\alpha + 2\sin^2\beta\cos\beta\sin 2\omega_0\langle\cos 2\Delta_1\rangle_{av}\langle\cos 2\Delta_{12}\rangle_{av} \times \sin 2\alpha\cos 2\alpha + \sin^4\beta\sin^2 2\alpha] \quad \text{(A-8)}$$

Integration over β leads to the result

$$\frac{1}{2\pi}\int_{\beta=0}^{2\pi}\langle(\mathbf{M}\cdot\mathbf{O})_1(\mathbf{M}\cdot\mathbf{O})_2\rangle_{r_{12}}\,d\beta =$$
$$\tfrac{1}{16}(\Omega_1\sin^2 2\alpha + 4\Omega_2\cos^2 2\alpha + \Omega_3\sin^2 2\alpha)f(r_{12}) + \tfrac{1}{16}(\Omega_3+\Omega_4)\sin^2 2\alpha \quad \text{(A-9)}$$

Substituting eq A-7 and A-9 into eq A-5, we obtain eq 2. We must also carry out the same calculations discussed above in the case of $r_1 > r_2$. That is, the scattered intensity obtained from the above calculations must be indicated

as the summation of the result in the case of $r_2 \geq r_1$ and that in the case of $r_1 > r_2$.

References and Notes

(1) Presented in part at the 28th Annual Meeting of the Society of Polymer Science, Japan, Tokyo, May 1979. (b) Yamagata University. (c) Nara Women's University.
(2) Toth, W. J.; Tobolsky, A. V. *J. Polym. Sci., Polym. Lett. Ed.* **1970**, *8*, 531.
(3) Stamatoff, J. B. *Mol. Cryst. Liq. Cryst.* **1972**, *16*, 137.
(4) Iizuka, E. *Biochim. Biophys. Acta* **1969**, *175*, 457.
(5) Iizuka, E. *Biochim. Biophys. Acta* **1971**, *243*, 1.
(6) Iizuka, E.; Keira, T.; Wada, A. *Mol. Cryst. Liq. Cryst.* **1973**, *23*, 13.
(7) Williams, R. *J. Chem. Phys.* **1963**, *39*, 384.
(8) Heilmeier, G. H. *J. Chem. Phys.* **1963**, *44*, 644.
(9) Tsuboi, M. *J. Polym. Sci.* **1962**, *59*, 139.
(10) O'Konski, C. T.; Yoshioka, K.; Orttung, W. H. *J. Phys. Chem.* **1959**, *63*, 1558.
(11) Watanabe, H.; Yoshioka, K.; Wada, A. *Biopolymers* **1964**, *2*, 91.
(12) Sobajima, S. *J. Phys. Soc. Jpn.* **1967**, *23*, 1070.
(13) Orwell, R. D.; Vold, R. L. *J. Am. Chem. Soc.* **1971**, *93*, 5335.
(14) Iizuka, E.; Go, Y. *J. Phys. Soc. Jpn.* **1971**, *31*, 1205.
(15) Samulski, E. T.; Tobolsky, A. V. *Macromolecules* **1968**, *1*, 555.
(16) Wilkes, G. L. *Mol. Cryst. Liq. Cryst.* **1972**, *18*, 165.
(17) Robinson, C. *Trans. Faraday Soc.* **1956**, *52*, 571.
(18) Robinson, C.; Ward, J. C.; Beevers, R. B. *Discuss. Faraday Soc.* **1958**, *25*, 29.
(19) Robinson, C. *Tetrahedron* **1961**, *13*, 219.
(20) Rhodes, M. B.; Stein, R. S. *J. Polym. Sci., Part A-2* **1969**, *7*, 1539.
(21) Stein, R. S.; Rhodes, M. B. *J. Appl. Phys.* **1960**, *31*, 1873.
(22) Stein, R. S.; Wilson, P. R. *J. Appl. Phys.* **1962**, *33*, 1914.
(23) Clough, S.; van Aartsen, J. J.; Stein, R. S. *J. Appl. Phys.* **1965**, *36*, 3072.
(24) Stein, R. S.; Erhardt, P. F.; Clough, S. B.; Adams, G. *J. Appl. Phys.* **1966**, *37*, 3980.
(25) Rhodes, M. B.; Porter, R. S.; Chu, W.; Stein, R. S. In "Liquid Crystals"; Gordon and Breach Science Publishers: New York, 1969; Vol. II.
(26) Picot, C.; Stein, R. S. *J. Polym. Sci., Part A-2* **1970**, *8*, 1491.
(27) Stein, R. S.; Chu, W. *J. Polym. Sci., Part A-2* **1970**, *8*, 1137.
(28) Hashimoto, T.; Stein, R. S. *J. Polym. Sci., Part A-2* **1971**, *9*, 1747.
(29) Stein, R. S.; Hashimoto, T. *J. Polym. Sci., Part A-2* **1971**, *9*, 517.
(30) Hashimoto, T.; Murakami, Y.; Hayashi, N.; Kawai, H. *Polym. J.* **1974**, *6*, 132.
(31) Hayashi, N.; Murakami, Y.; Moritani, M.; Hashimoto, T.; Kawai, H. *Polym. J.* **1973**, *4*, 560.

Neutron Scattering Studies on the Conformation of Atactic Polystyrene Chains in a Bulk-Crystallized Isotactic Polystyrene

Jean-Michel Guenet* and Claude Picot

Centre de Recherches sur les Macromolécules (CNRS), 67083 Strasbourg Cedex, France.

Received February 12, 1980

ABSTRACT: The conformation of atactic polystyrene in a semicrystalline isotactic polystyrene matrix has been determined through the use of small-angle neutron scattering. Keeping the concentration of the deuterated atactic species constant ($C_D \sim 1\%$), we have systematically varied the degree of crystallinity of the sample by two methods: (1) by annealing the samples for different times at $T_c = 180$ °C (system A); (2) by introducing increasing amounts of hydrogenated atactic polystyrene and keeping the annealing time constant (system B). In system A, the results show that chains are excluded from the crystallizing regions for low crystallinities. For the highest crystallinities, the experimental results suggest that the chains are trapped and extended within the fibrils and the short-range structure is far from the Gaussian. In system B, the chains remain elongated but the subunits recover their Gaussian statistic. Viscoelastic properties of melt polymers are used to provide explanations for these results, which are also discussed in regard to other works performed on similar samples.

Introduction

Many papers have been devoted to the rejection of noncrystallizable materials during the crystallization process of stereoregular polymers.[1-6] For example, the stereoirregular structure of atactic polystyrene (APS) not only hinders its crystallization but also makes it unlikely that it can be incorporated, to any significant extent, within the crystals of the corresponding stereoregular polymer. Some years ago, Keith and Padden[1] studied by optical microscopy the spherulitic structure of the same system. By modifying the content of impurities (i.e., APS content) in a blend with isotactic polystyrene (IPS), they showed that the interfibrillar melt is composed of mainly atactic material which has been rejected at the tips of the growing fibers.

These interpretations are in agreement with those given by Yeh and Lambert[2] based on kinetic studies. These authors concluded, by measuring the variations in spherulitic growth rate as a function of molecular weight of the atactic species, that above $M_w = 5 \times 10^4$ significant amounts of noncrystallizable rejected chains are trapped within the growing spherulites and that they probably reside in the interfibrillar domain as opposed to the interlamellar regions.

More recently, Stein and co-workers[3] examined the lamellar structure in these blends by small-angle X-ray scattering (SAXS). Upon addition of the atactic "impurity", they found an invariance of the interlamellar distance as well as an invariance in lamellar stacking parameters as ascertained by application of the Hosemann paracrystalline model.[7] In view of these results, they concluded that the findings of Keith and Padden and Yeh and Lambert are qualitatively correct. That is, since rejected material is not incorporated into the interlamellar regions, it must be included in the interfibrillar melt.

The purpose of this paper is to extend these previous works to the determination of the chain conformation of the rejected species, which may be accomplished through the use of small-angle neutron scattering (SANS). With this technique, a small amount of the atactic chains may be preferentially deuterium labeled, which allows their isolated behavior to be determined directly in the bulk state.[8,9] This paper will examine the effects of both annealing time and addition of hydrogenated atactic species on the conformation of deuterated atactic polystyrene chains in the bulk blend with isotactic polystyrene.

Sample Preparation and Description

Isotactic polystyrene was synthesized at 80 °C in heptane with $Al(C_2H_5)_3$–$TiCl_4$ as catalyst according to the well-known Natta method.[10] After extraction of the atactic material in boiling heptane and in methyl ethyl ketone, the molecular weights deduced from GPC[11] were $M_w = 8.75 \times 10^5$ and $M_n = 1.5 \times 10^5$.

0024-9297/81/2214-0309$01.25/0